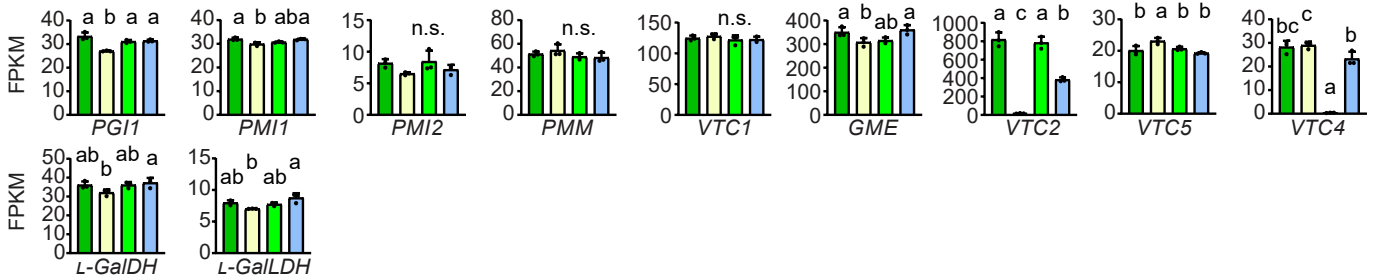


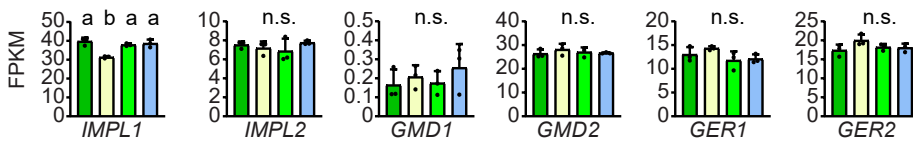
Supplementary Figure S1. Expression of genes related to ascorbate homeostasis in four-week-old rosettes. Individual gene plots are available in Supplementary Fig. S2. Continuous black lines show the enzyme-catalyzed conversion steps whose corresponding genes are represented in the bar chart. Grey lines represent steps not depicted, and dotted lines indicate possible conversion routes. Bar charts represent mean values and error bars their corresponding standard deviations. Different letters denote statistically significant differences (One-Way ANOVA, Tukey post-hoc test, $\alpha=0.05$, $n=3$). Distributions were tested to meet normality (Shapiro–Wilk’s test) and homoscedasticity (Levene’s test) prior to ANOVA. If not meeting any of these requirements, data was transformed using logarithm and, if meeting the requirements, we proceeded to perform ANOVA. Otherwise, Kruskal-Wallis followed by Dunn’s post-hoc test were performed. *IMPL1*: MYO-INOSITOL MONOPHOSPHATASE LIKE 1. *IMPL2/HISN7*: MYO-INOSITOL MONOPHOSPHATASE LIKE 2/HISTIDINE BIOSYNTHESIS 7, *GMD1*: GDP-D-MANNOSE-4,6-DEHYDRATASE 1; *GER1*: GDP-4-KETO-6-DEOXYMANNANOSE-3,5-EPIMERASE-4-REDUCTASE, *GalUR*: D-GALACTURONATE ACID REDUCTASE. *APX*: ASCORBATE PEROXIDASE (*tAPX*: tylakoidal APX, *sAPX*: stromatic APX), *AO*: ASCORBATE OXIDASE, *MDHAR*, MONODEHYDROASCORBATE REDUCTASE; *DHAR*, DEHYDROASCORBATE REDUCTASE, *KJC1*: KONJAC1, *CML10*: CALMODULIN-LIKE10, *CSN1*: COP9 SIGNALOSOME COMPLEX SUBUNIT 1, *PHT4.4*: INORGANIC PHOSPHATE TRANSPORTER, *VTC3*: DUAL FUNCTION PROTEIN KINASE::PROTEIN PHOSPHATASE. FPKM: Fragments Per Kilobase of transcript per Million mapped reads

■ WT ■ *vtc2* ■ *vtc4* ■ *vtc2/OE-VTC2*

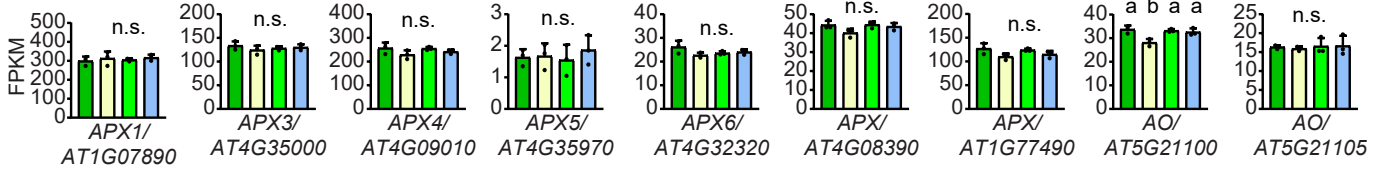
L-Ascorbate main biosynthesis pathway (Smirnoff-Wheeler)



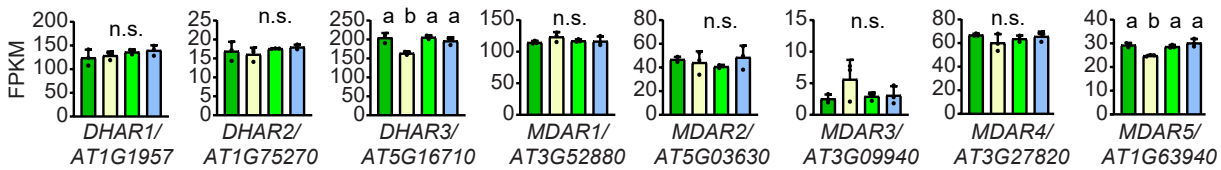
Other biosynthesis pathways



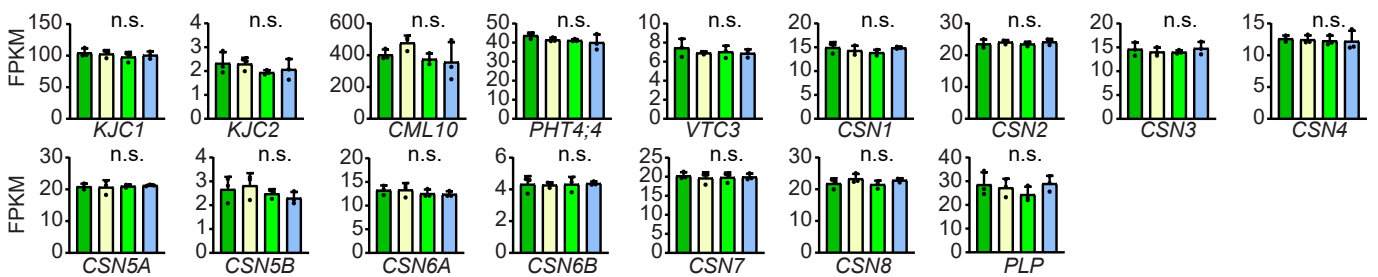
Catabolism



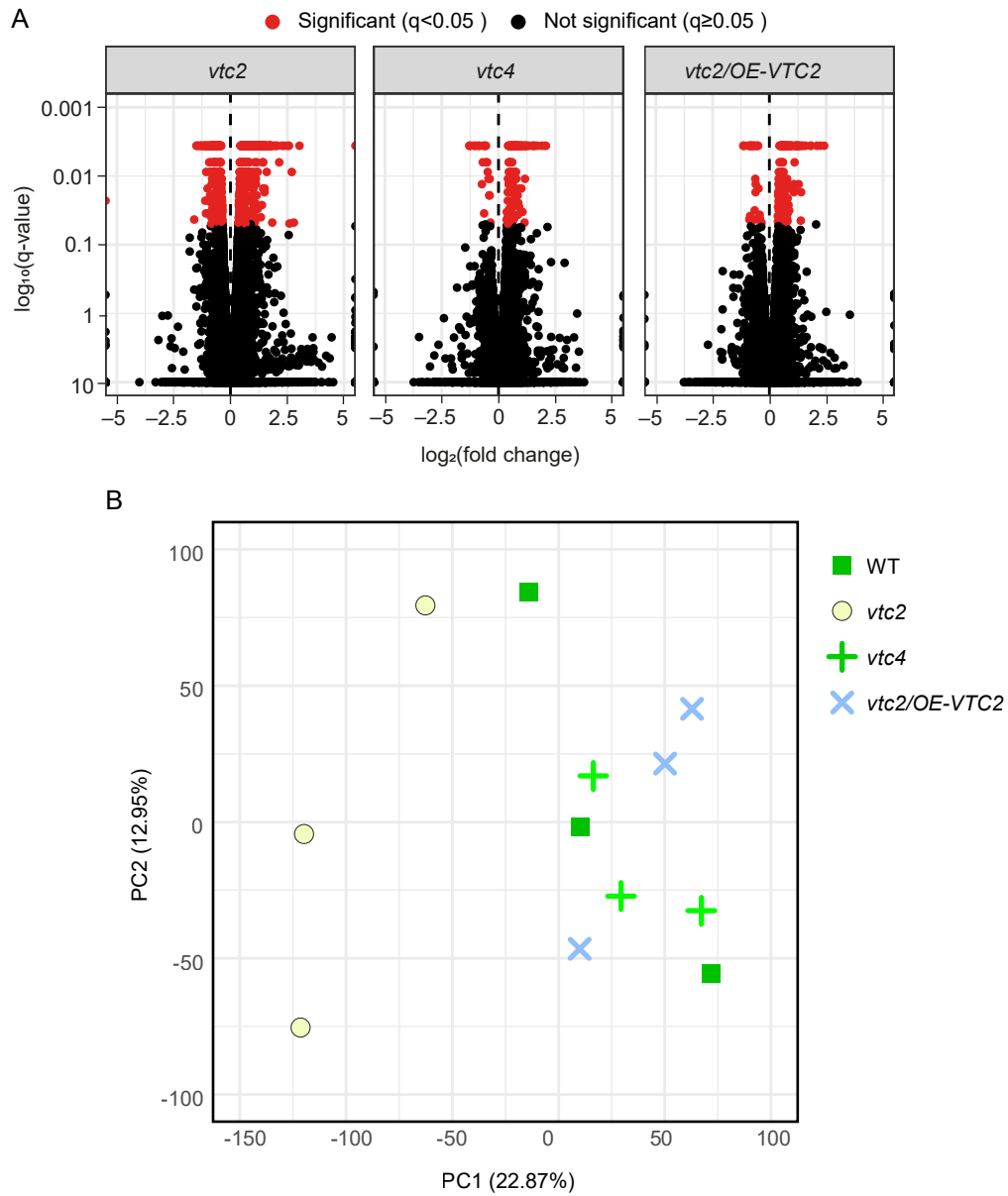
Recycling



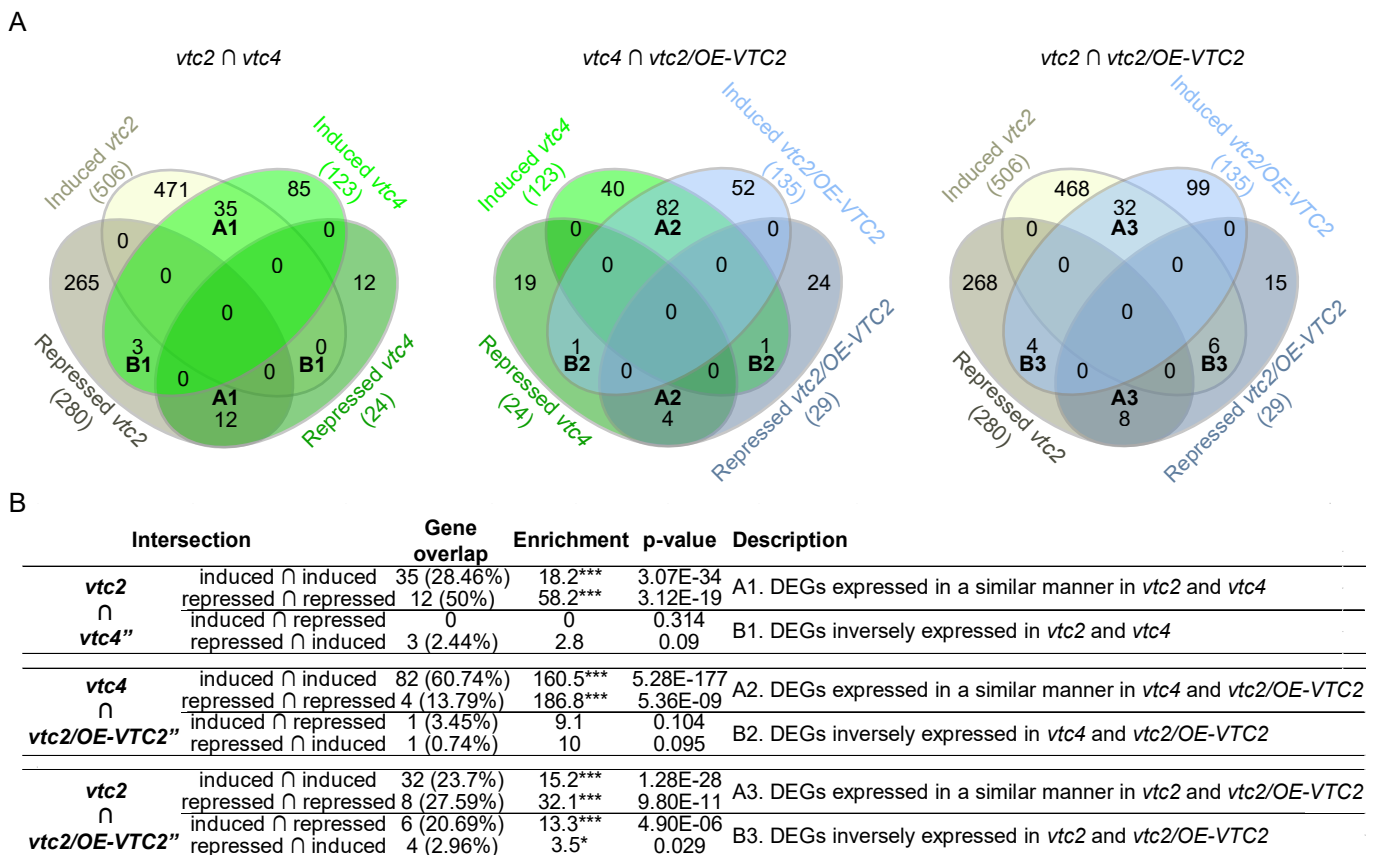
Regulators



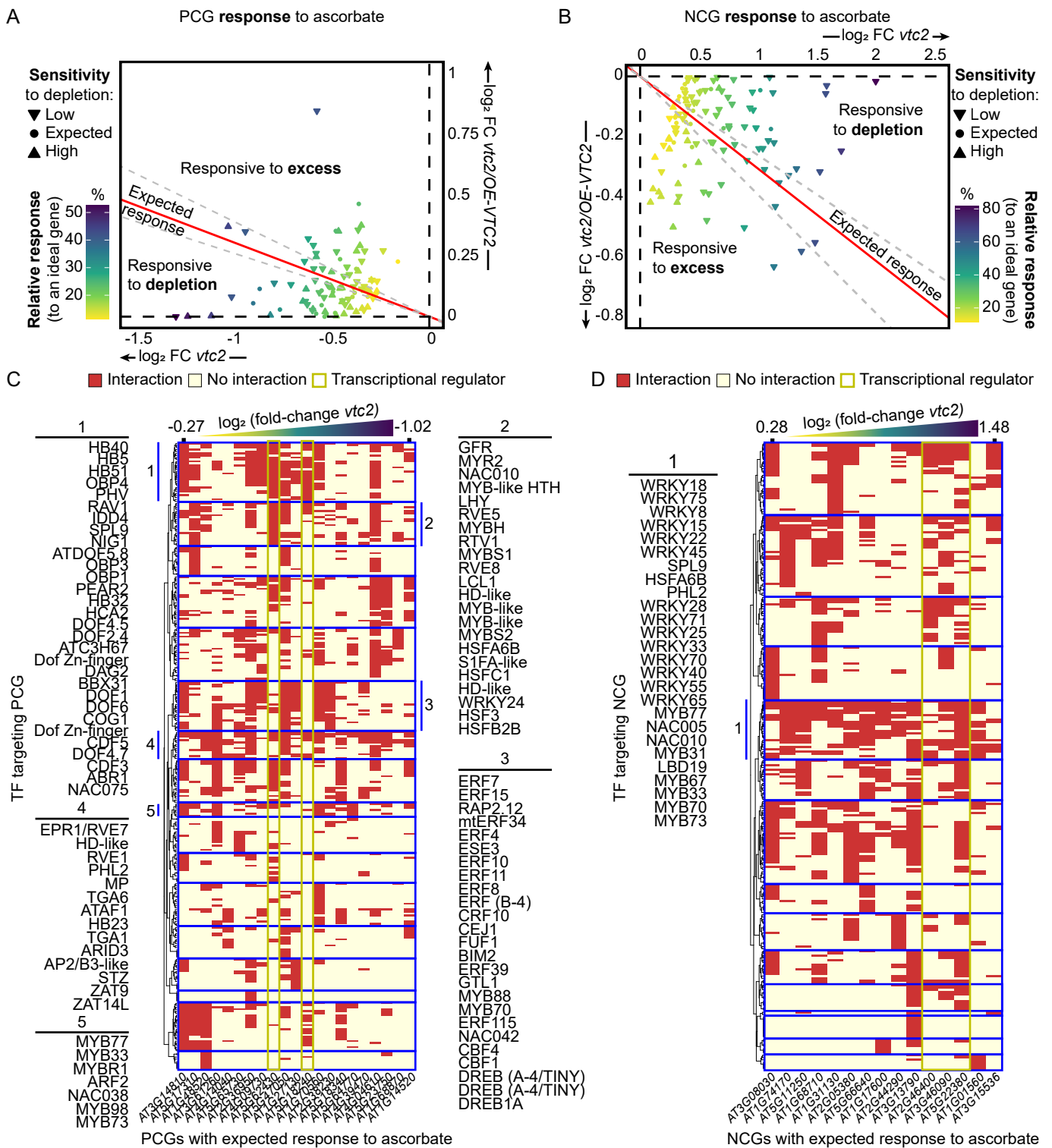
Supplementary Figure S2. Expression of individual genes related to ascorbate homeostasis in four-week-old rosettes. Bar charts represent mean values and error bars their corresponding standard deviations. Different letters denote statistically significant differences (One-Way ANOVA, Tukey post-hoc test, $\alpha=0.05$, $n=3$). Distributions were tested to meet normality (Shapiro-Wilk's test) and homoscedasticity (Levene's test) prior to ANOVA. If not meeting any of these requirements, data was transformed using logarithm and, if meeting the requirements, proceeded to perform ANOVA. Otherwise, Kruskal-Wallis followed by Dunn's post-hoc test were performed. *PMI*: PHOSPHOMANNOSE ISOMERASE, *PMM*: PHOSPHOMANNOMUTASE, *VTC1*: VITAMIN C DEFICIENT1 (GDP-D-MANNOSE PYROPHOSPHORYLASE), *GME*: GDP-D-MANNOSE-3',5'-ISOMERASE, *VTC2*: GDP-L-GALACTOSE PHOSPHORYLASE, *VTC4*: L-GALACTOSE-1-PHOSPHATE PHOSPHATASE, *L-GalDH*: L-GALACTOSE DEHYDROGENASE, *L-GalLDH*: L-GALACTONO-1,4-LACTONE DEHYDROGENASE. *IMPL1*: MYO-INOSITOL MONOPHOSPHATASE LIKE 1. *IMPL2/HISN7*: MYO-INOSITOL MONOPHOSPHATASE LIKE 2/HISTIDINE BIOSYNTHESIS 7, *GMD1*: GDP-D-MANNOSE-4,6-DEHYDRATASE 1; *GER1*: GDP-4-KETO-6-DEOXYMANNOSE-3,5-EPIMERASE-4-REDUCTASE. *APX*: ASCORBATE PEROXIDASE, *AO*: ASCORBATE OXIDASE, *MDAR*, MONODEHYDROASCORBATE REDUCTASE; *DHAR*, DEHYDROASCORBATE REDUCTASE, *KJC1*: KONJAC1, *CML10*: CALMODULIN-LIKE10, *PHT4.4*: INORGANIC PHOSPHATE TRANSPORTER, *VTC3*: DUAL FUNCTION PROTEIN KINASE::PROTEIN PHOSPHATASE, *CSN1*: COP9 SIGNALOSOME COMPLEX SUBUNIT 1, *PLP*: PAS/LOV (Per-ARNT-Sim/Light-Oxygen-Voltage) PROTEIN. FPKM: Fragments Per Kilobase of transcript per Million mapped reads



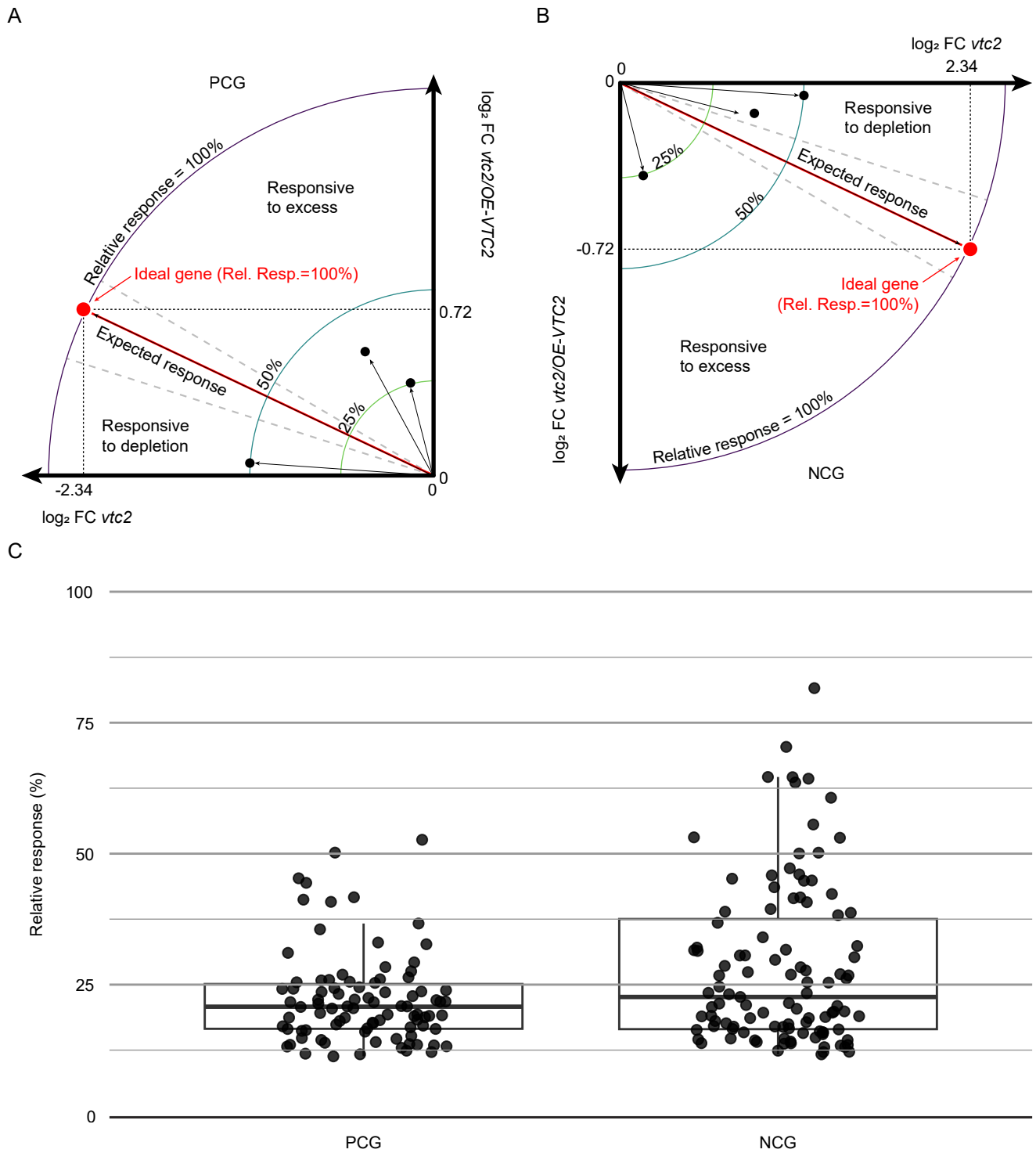
Supplementary Figure S3. Transcriptome profiles of four-week-old Arabidopsis rosettes with altered concentrations of endogenous ascorbate. A) Volcano plots showing that the statistically significant DEGs (red) are more abundant in *vtc2* compared to *vtc4* or *vtc2/OE-VTC2*. Fold change between each ascorbate mutant and WT is presented in log₂ scale, whereas FDR-corrected p-values (q-values) are presented in log₁₀ scale. Significance cutoff was set at $\alpha=0.05$. Among Differentially expressed genes (DEGs) ($q\text{-value} < 0.05$, red dots) across genotypes, the smallest log₂(fold-change)=0.33 (1.25-fold) for the induced genes and -0.33 (0.8-fold) for repressed genes. B) Principal Component Analysis plot displaying all replicates for each of the four genotypes.



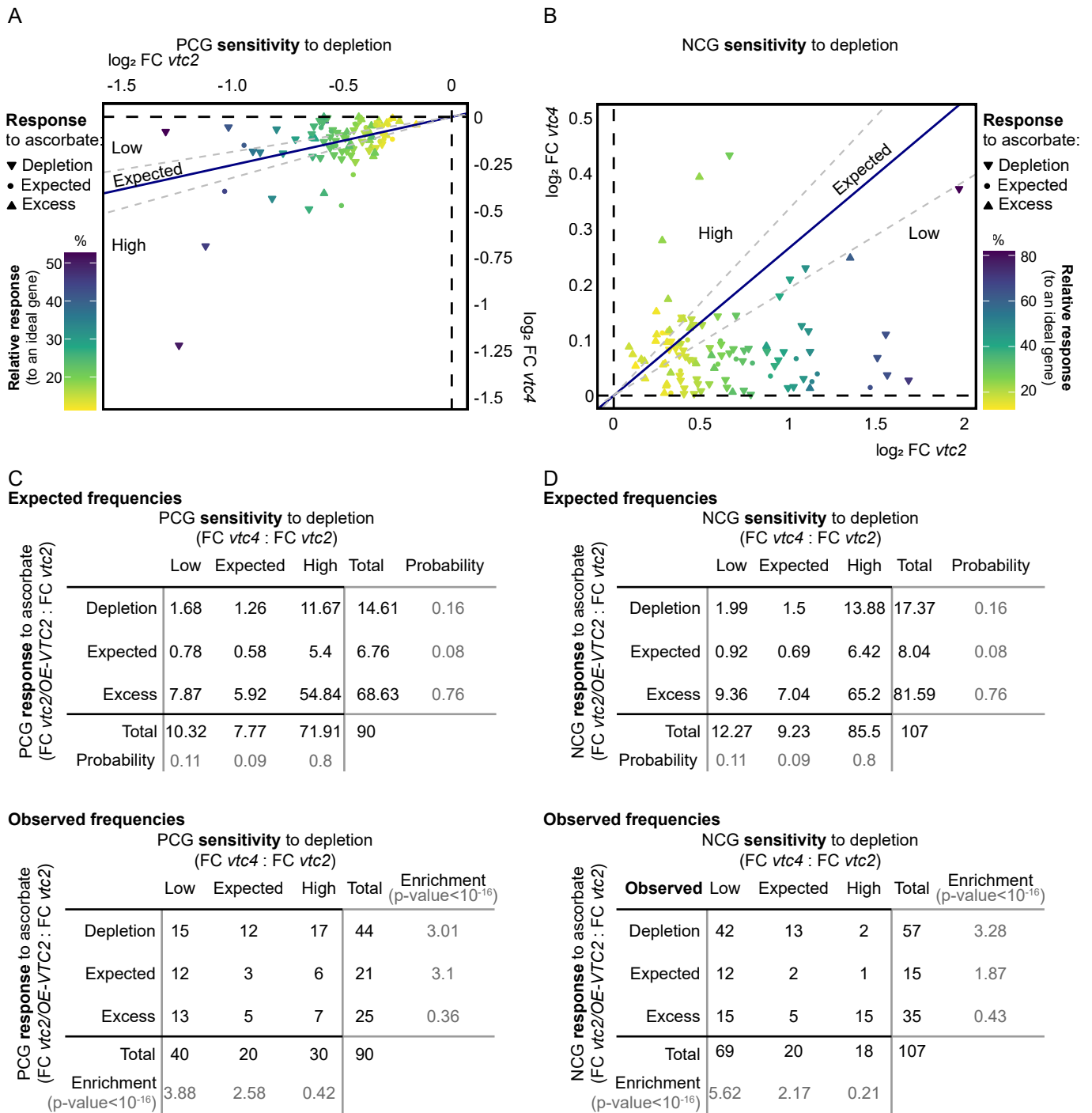
Supplementary Figure S4. Shared and Line-Specific Transcriptional Responses in Ascorbate-Altered Arabidopsis Lines. A) Venn diagrams depicting the pairwise overlap of DEGs between four-week-old Arabidopsis rosettes of ascorbate-altered lines. A) Absolute number of genes overlapping between two plant lines. The \cap symbol denotes intersection. For any two sets of X and Y, $X \cap Y$ is read as X intersection with Y. Group names A1-A3 and B2-B3 are described in B). B) Statistical analysis of the DEG overlap. The percentage of the overlapped genes was calculated by dividing the number of overlapped genes by the number of genes in the genotype marked with the symbol (") and multiplied by 100. The enrichment is calculated by dividing the number of overlapping genes by the expected number of overlapping genes (if the overlap was random) drawn from two independent groups. Therefore, values >1 denote more overlap than expected, <1 less overlap than expected and, $=1$ indicates the expected overlap between two independent groups of genes. Level of statistical significance of the overlap is noted as * (p-value <0.05) and *** (p-value <0.001).



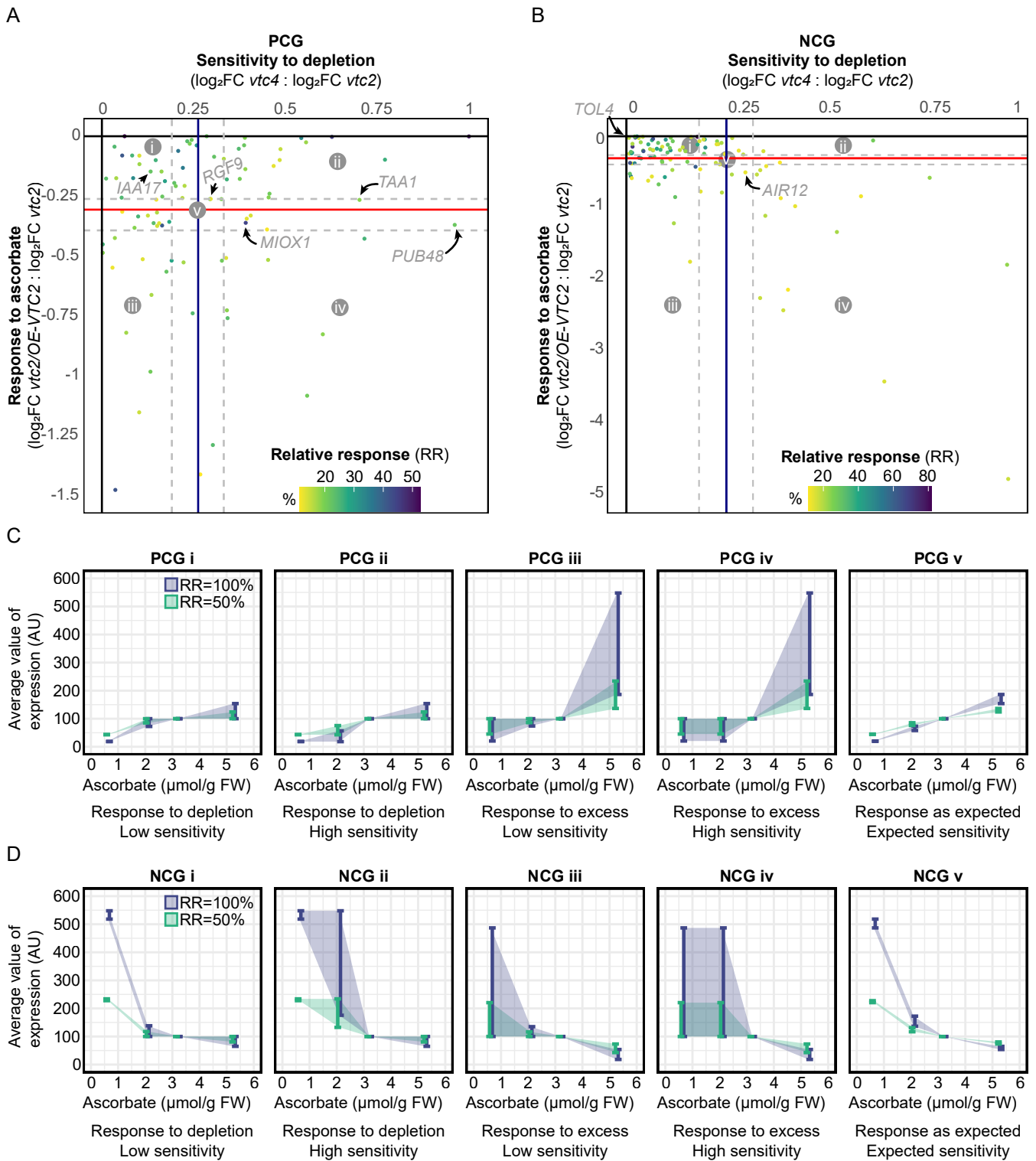
Supplementary Figure S5. Ascorbate-correlated genes in four-week-old rosettes show different types of response to ascorbate concentration. A) Positively correlated genes (PCGs). B) Negatively correlated genes (NCGs). To establish the identity of the plot area, the following scenarios were considered: a theoretical gene would experience a 1:1 change in expression following a change in ascorbate concentration. Thus, this ideal PCG would be 5-fold repressed in *vtc2* (20% of WT ascorbate content), and 1.65-fold induced in *vtc2/OE-VTC2* (165% of WT ascorbate content), whereas an ideal NCG would be 5-fold induced in *vtc2* and 1.65-fold repressed in *vtc2/OE-VTC2*. Taking \log_2 , these fold changes would be -2.34 for *vtc2* and 0.72 for *vtc2/OE-VTC2* (PCG) or 2.34 and -0.72, respectively, as an NCG, hence defining the coordinates for an ideal PCG (-2.34, 0.72) and for an ideal NCG (2.34, -0.72). The line that links these point with the (0,0) defines the ideal proportion in the change of expression given the change in ascorbate concentration. The distance between (0,0) and (2.34, -0.72) represents the 100% of a 1:1 response (see Supplementary Fig. S6 for further details). Genes whose expression is changed in both *vtc2* and *vtc2/OE-VTC2* lines following this proportion (i.e., $\log_2FC\ vtc2/OE-VTC2 : \log_2FC\ vtc2$ remains constant) are classified as correlated genes responding as expected and lay near the red line within the calculated error margins (gray dotted lines). In turn, a given gene with an expression FC *vtc2* close to 0 implies that a severe ascorbate depletion does not affect its expression, and therefore, its correlation with ascorbate concentration can only be by due to the response to ascorbate excess. Following the same rationale, correlated genes with FC *vtc2/OE-VTC2* close to 0 show WT levels of expression under the accumulation of ascorbate, and therefore, these genes are classified as responsive to ascorbate depletion. The symbols represent the sensitivity of a given gene to ascorbate depletion, calculated as $\log_2FC\ vtc4 : \log_2FC\ vtc2$, graphically represented in Supplementary Fig. S6. C, D) Transcription Factors (TF) interacting with the promoters of PCGs (C) and NCGs (D) with expected response (i.e., proportional to (-2.34, 0.72) or (2.34, 0.72)), extracted from O'Malley *et al.*, (2016) using methylated DNA as template. Detected interaction between the TF and the promoter of the gene is colored in red, whereas no interaction is colored in light yellow. Transcriptional regulators that are correlated to ascorbate concentration as expected are highlighted with a yellow rectangle. Targeted correlated genes are arranged from the mildest (left) to the strongest (right) expression fold-change in the *vtc2* mutant. TF clustering distances were calculated and plotted using Ward.D2 method in ComplexHeatmap R package (Gu *et al.*, 2016; Gu, 2022).



Supplementary Figure S6. Relative response of ascorbate correlated genes compared to an ideal ascorbate-regulated gene. A theoretical ideal gene would experience a change in expression proportional to the change in ascorbate concentration. A) A Positively Correlated Gene (PCG) responding 1:1 to ascorbate concentration would experience a 5-fold repression in *vtc2* (20% of WT ascorbate content) and a 1.65-fold induction in *vtc2*/OE-*VTC2* (165% of WT ascorbate content), whereas a B) Negatively Correlated Gene (NCG) would be 5-fold induced in *vtc2* and 1.65-fold repressed in *vtc2*/OE-*VTC2*. Taking log₂Fold change (FC) of *vtc2*'s and *vtc2*/OE-*VTC2*'s ascorbate concentration, an ideal PCG would lay on the (-2.32, 0.72) and an ideal NCG on the (2.32, -0.72). Hence, the distance between (0,0) and these two points set the 100% of a 1:1 response of gene expression to ascorbate concentration. C) Distribution of relative responses observed in ascorbate-correlated genes. We considered the distance between the ideal gene and the (0, 0) as the 100% relative response to ascorbate concentration (also noted as Rel. Resp.) and the relative response of all correlated genes (black thin arrows) were calculated using the Pythagorean theorem and normalized to the ideal gene. Each datapoint represents the relative response of an individual gene. Box-and-whisker plots display the median (center line), the interquartile range from the 25th to the 75th percentile (box), and the data range within 1.5× the interquartile range (whiskers); data points outside this range are shown as outliers.

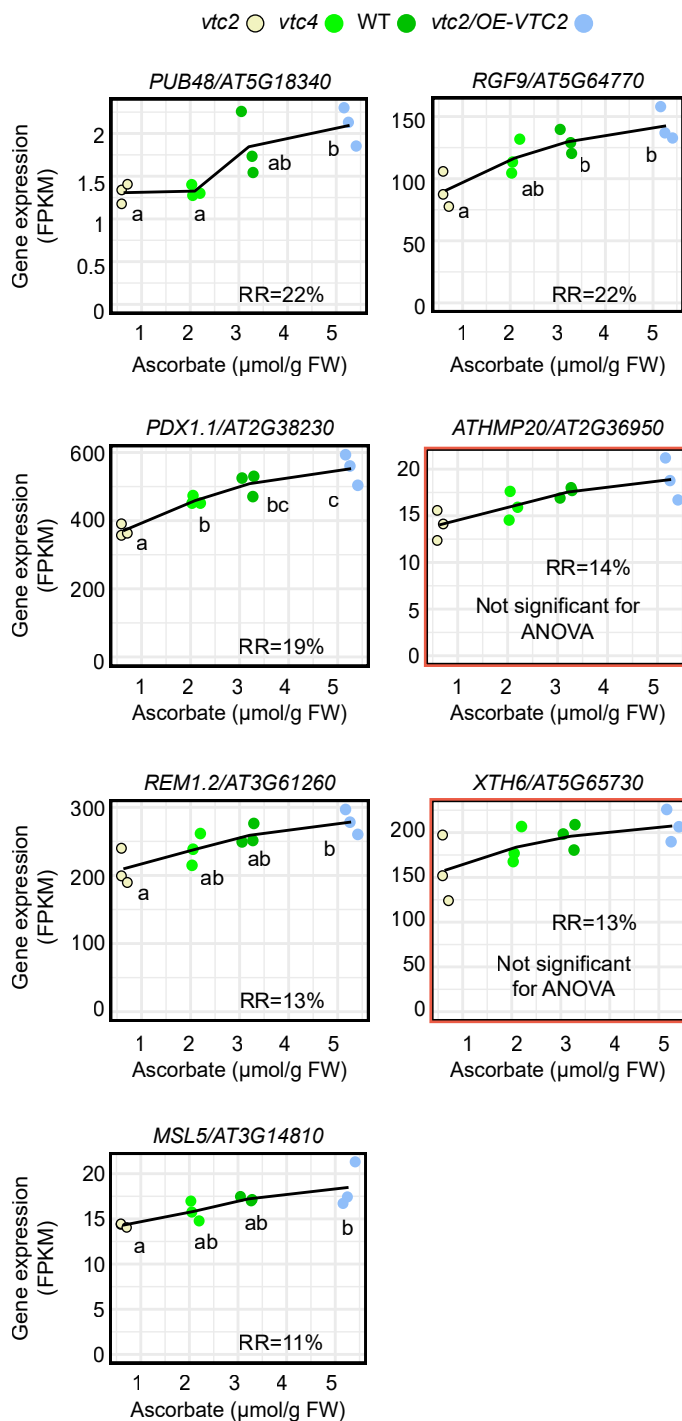


Supplementary Figure S7. Ascorbate-correlated genes in four-week-old rosettes are enriched in the response to depletion. Gene expression sensitivity to ascorbate depletion of A) PCGs and B) NCGs. To establish the identity of the plot area, we considered the following premises. A theoretical ideal gene would experience a change in expression proportional to the change in ascorbate concentration. An ideal PCG would be 5-fold repressed in *vtc2* (20% of WT ascorbate content), and 1.53-fold repressed in *vtc4* (65% of WT ascorbate content), whereas an ideal NCG would be 5-fold induced in *vtc2* and 1.53-fold induced in *vtc4*. Taking \log_2 Fold change (FC) of *vtc2*'s and *vtc4*'s ascorbate concentration, an ideal PCG would experience a change in expression that would be represented as point (-2.32, -0.61) and an ideal NCG as (2.32, 0.61). The navy-blue line represent all values that keep the \log_2 FC *vtc2* : \log_2 FC *vtc4* equal to 2.32/0.61. Therefore, those genes lying near the blue line within the error margins (gray dashed lines) are considered genes with an expected sensitivity to ascorbate depletion. Genes with a greater ratio experienced a greater-than-expected change in expression under a mild ascorbate deficiency (*vtc4*), and therefore, we considered these genes had high sensitivity to ascorbate depletion. Conversely, genes whose expression FC in *vtc4* is closer to 0 would represent genes that remained unaltered under mild ascorbate deficiency, and therefore, they are classified as genes with low sensitivity to ascorbate depletion. C,D) Expected (top panel) and observed (lower panel) frequencies of PCGs (C) and NCGs (D) belonging to each category of response to ascorbate (based on \log_2 FC *vtc2*/OE-*VTC2* : \log_2 FC *vtc2*, see Supplementary Fig. S5) and sensitivity to its depletion (\log_2 FC *vtc2* : \log_2 FC *vtc4*), also available in Supplementary Dataset S6A-B. The enrichment is calculated as the total number of observed genes belonging to a category divided by the total number of expected genes belonging to the same category. The expected number of genes for a given category were calculated multiplying the probability of belonging to that category by chance by the total number of PCGs (90) or NCGs (107). The probability of belonging to a given category by chance was calculated using a Monte Carlo approach based on the proportion that each category takes in the plot. To do that, a blank plot with equal-length axes containing the "expected" area was printed and proportions were estimated based on weight using a precision scale. To guarantee accuracy in the proportions, a circular line whose radius equals the length of the axes was inscribed to ensure that probabilities estimated consider genes with the same relative response.

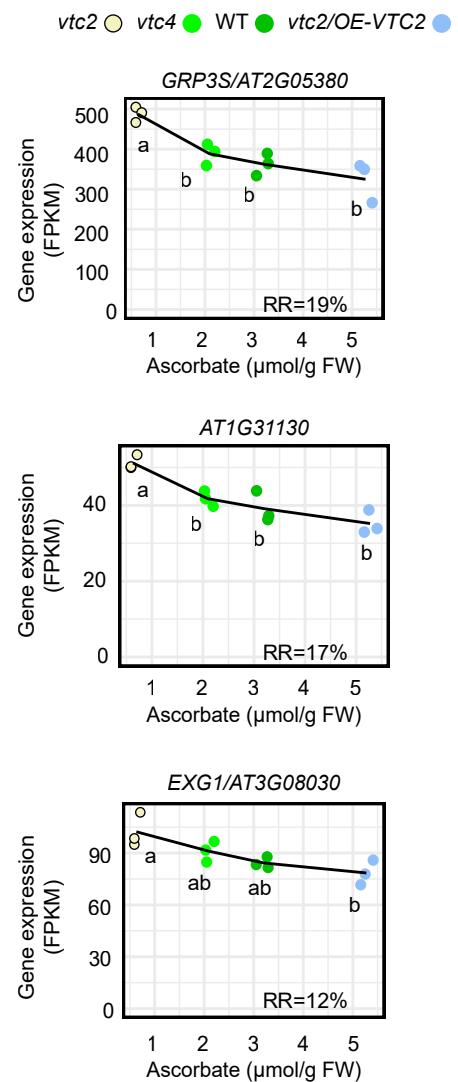


Supplementary Figure S8. The expression patterns of ascorbate-correlated genes. A) Positively Correlated Genes (PCGs). B) Negatively Correlated Genes (NCGs). The y-axis represents a gene's response to changes in ascorbate concentration and it is obtained from Supplementary Fig. S5A and B by dividing gene expression FC in *vtc2/OE-VTC2* by that in *vtc2*. The x-axis represents a gene's sensitivity to ascorbate depletion, and it is obtained from Supplementary Fig. S7A and B by dividing a gene's expression FC in *vtc4* by that in *vtc2*. To establish the identity of the plot area, the following scenarios were considered. A theoretical ideal gene would experience a change in expression proportional to the change in ascorbate concentration. Thus, the expression FC of an ideal PCG would be 0.2 in *vtc2*, 0.65 in *vtc4*, and 1.65 in *vtc2/OE-VTC2*, whereas for an ideal NCG it would be 5, 1.53, and 0.61 for *vtc2*, *vtc4*, and *vtc2/OE-VTC2*, respectively. Therefore, after taking \log_2 , an ideal gene would show a $FC_{vtc2/OE-VTC2} : FC_{vtc2} = -0.31$ (horizontal red line) and a $FC_{vtc4} : FC_{vtc2} = 0.26$ (vertical navy-blue line). Thus, the horizontal red line intersecting the y-axis and the dashed gray horizontal lines represent the expected response and the error margins of calculation, respectively (like in Supplementary Fig. S5A and B), and the vertical navy-blue line represents the expected sensitivity of a gene (like in Supplementary Fig. S7A and B). C, D) Theoretical expression intervals were calculated to illustrate the expected mean expression (arbitrary units, AU) of a hypothetical gene in response to ascorbate, relative to WT (set at 100 FPKM). The bar limits are calculated based on the sector they lay in—PCG (C) or NCG (D)—and by assuming either a 50% or 100% relative response (RR), defined as the fold-change in gene expression divided by the fold-change in ascorbate concentration. *IAA17*: *INDOLE-3-ACETIC ACID INDUCIBLE 17* (*AT1G04250*), *RGF9*: *ROOT MERISTEM GROWTH FACTOR 9* (*AT5G64770*), *MIOX1*: *MYO-INOSITOL OXYGENASE 1* (*AT1G14520*), *TAA1*: *TRYPTOPHAN AMINOTRANSFERASE OF ARABIDOPSIS 1* (*AT1G70560*), *PUB48*: *PLANT U-BOX 48* (*AT5G18340*), *TOL4*: *TOM1-LIKE 4* (*AT1G76970*), *AIR12*: *AUXIN-INDUCED IN ROOT CULTURES 12* (*AT3G07390*).

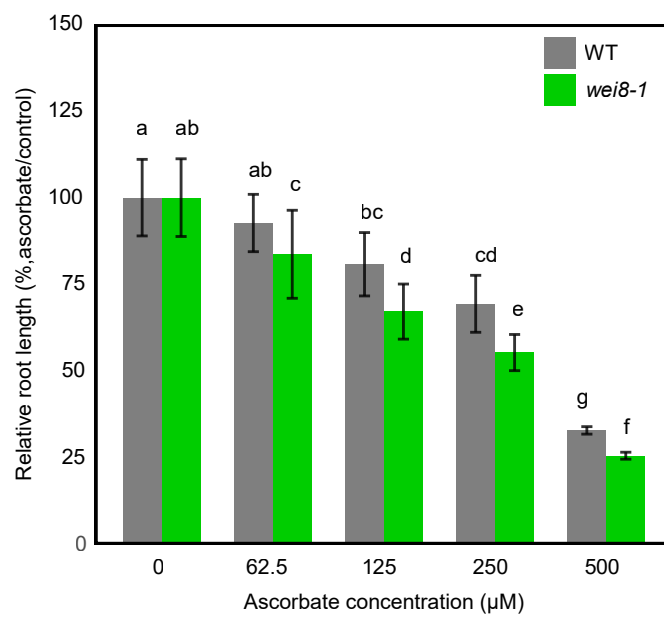
A



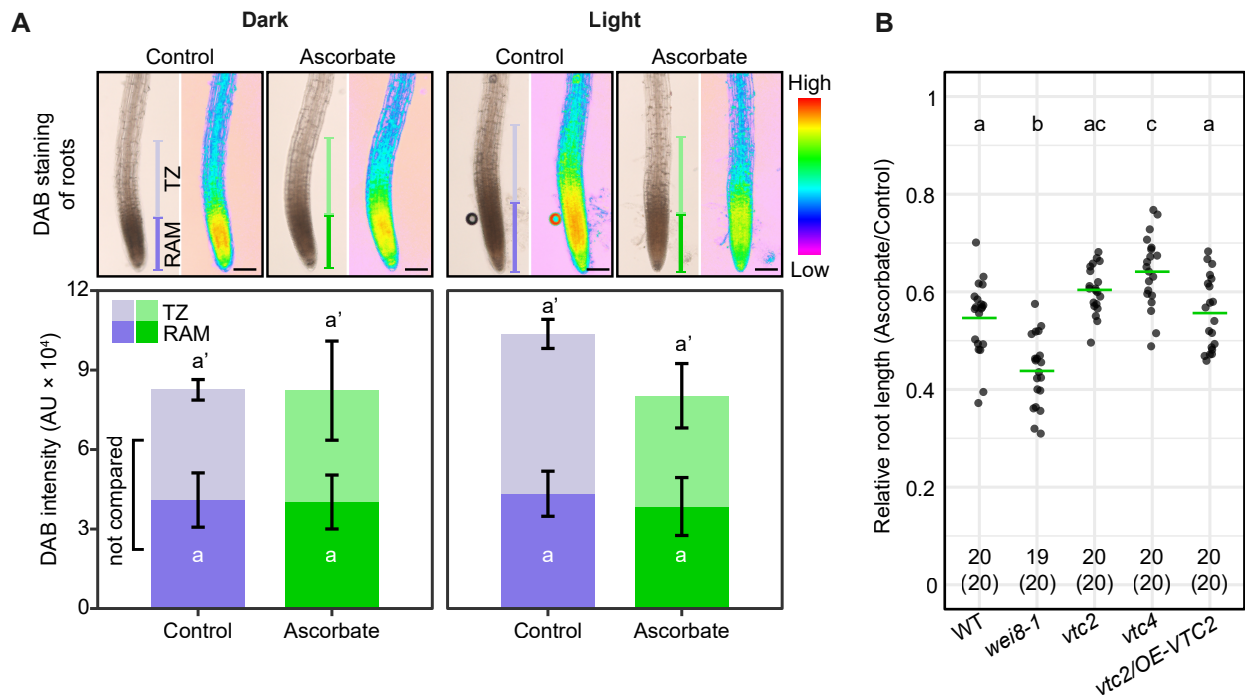
B



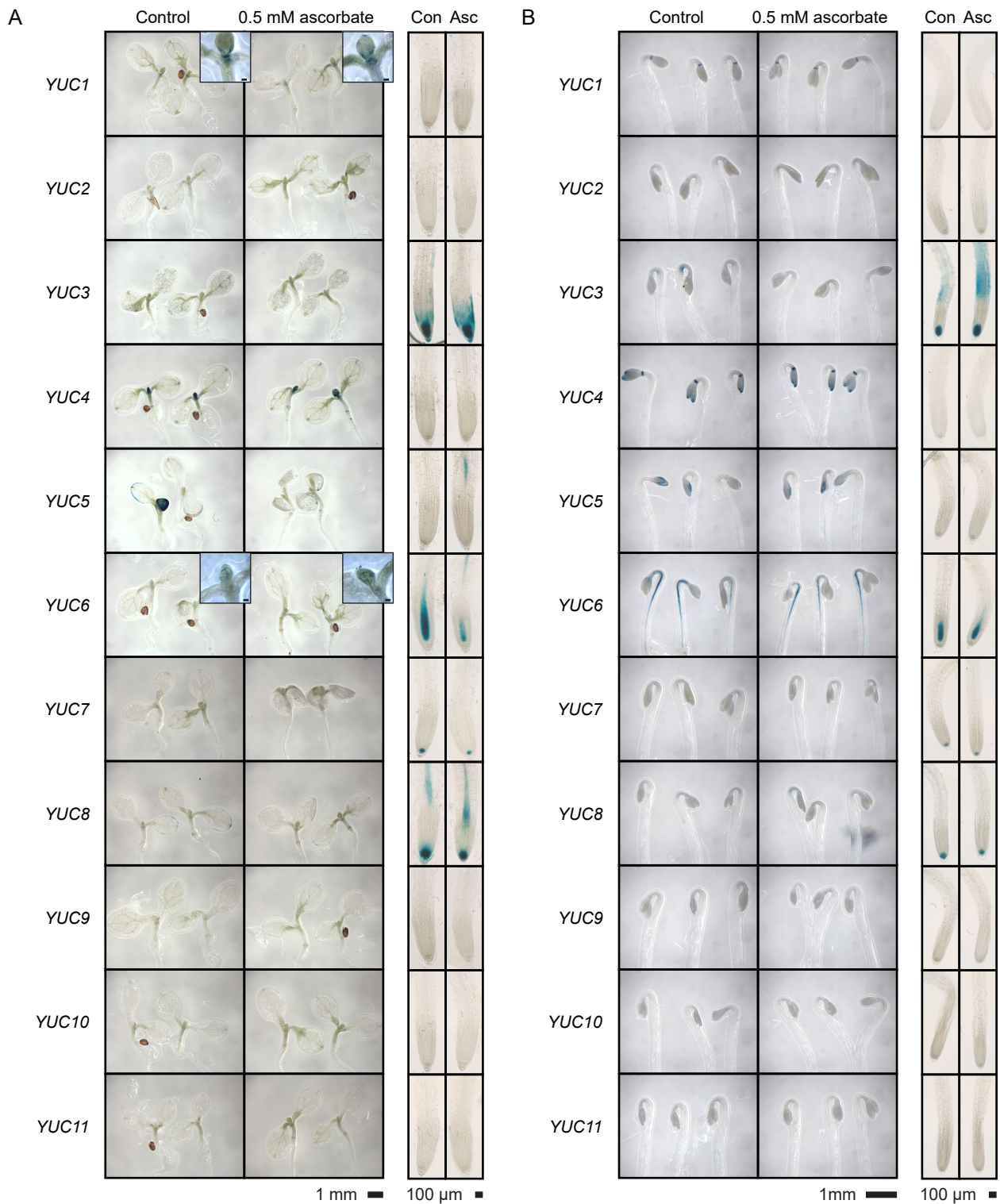
Supplementary Figure S9. Transcriptional responses of ascorbate-sensitive Positively and Negatively Correlated Genes in four-week-old Arabidopsis rosettes. Expression profiles of A) Positively Correlated Genes (PCGs) and B) Negatively Correlated Genes (NCGs) showing a response to ascorbate “as expected” with either “expected” or “high” sensitivity to ascorbate depletion (defined as FC *vtc4* : FC *vtc2*). Different letters denote statistically significant differences (One-Way ANOVA, Tukey post-hoc test, $\alpha=0.05$, $n=3$). Distributions were tested to meet normality (Shapiro–Wilk’s test) and homoscedasticity (Levene’s test) prior to ANOVA. If not meeting any of these requirements, data was transformed using logarithm and, if meeting the requirements, proceeded to perform ANOVA. Otherwise, Kruskal–Wallis followed by Dunn’s post-hoc test were performed. FPKM: Fragments Per Kilobase of transcript per Million mapped reads, FW: fresh weight, RR: relative response as defined in Supplementary Fig. S6, *PUB48*: PLANT U-BOX 48, *RGF9*: ROOT MERISTEM GROWTH FACTOR 9, *PDX1.1*: PYRIDOXINE BIOSYNTHESIS 1.1, *XTH6*: XYLOGLUCAN ENDOTRANSGLUCOSYLASE/HYDROLASE 6, *MSL5*: MECHANOSENSITIVE CHANNEL OF SMALL CONDUCTANCE-LIKE 5, *ATHMP20*: HEAVY METAL ASSOCIATED PROTEIN 20, *REM1.2*: REMORIN 1.2, *AT1G31130*: POLYADENYLATE-BINDING PROTEIN 1-B-BINDING PROTEIN, *GRP3S*: GLYCINE-RICH PROTEIN 3 SHORT ISOFORM, *EXG1*: ENHANCED XYLEM AND GRAFTING 1.



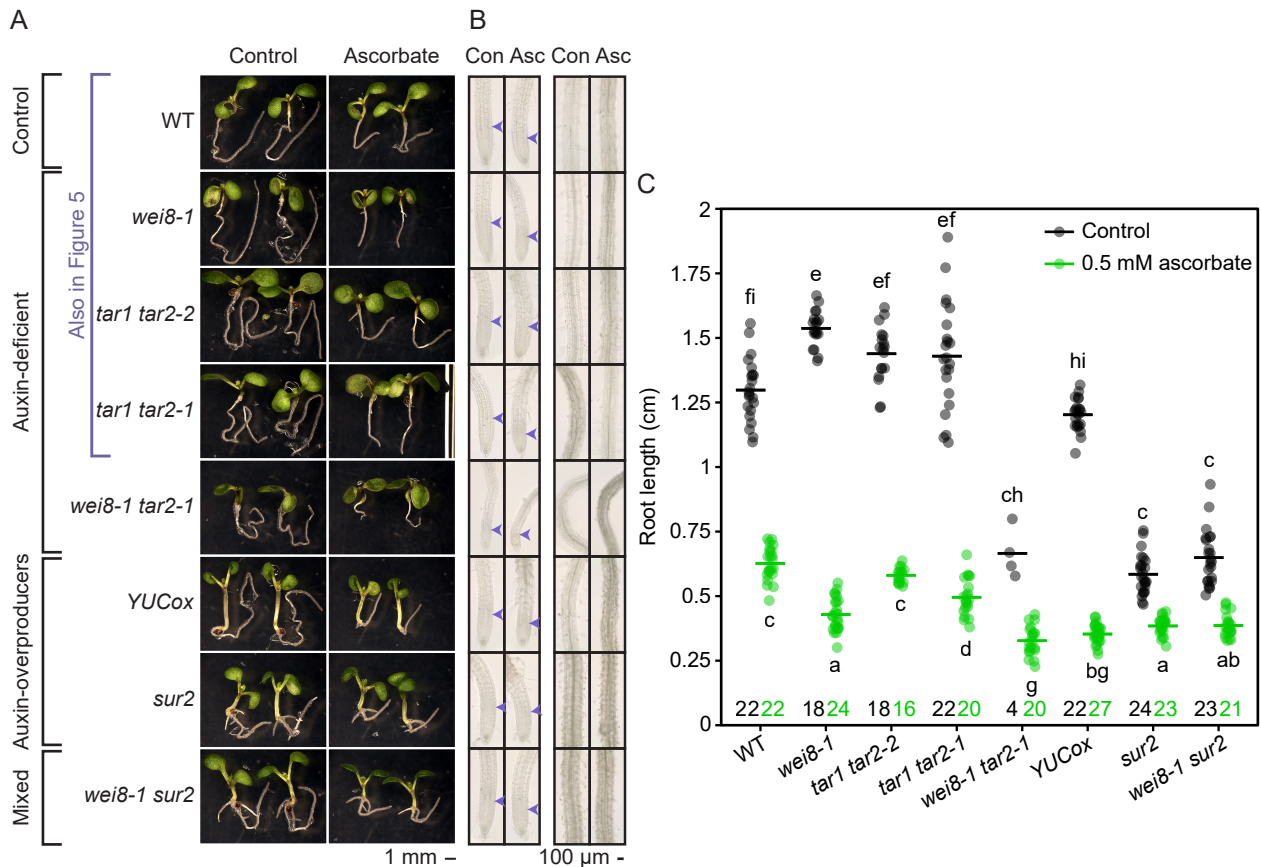
Supplementary Figure S11. Root sensitivity of mild auxin deficient mutant *wei8* to exogenous ascorbate is higher than WT in five-day-old light-grown seedlings. Roots of five-day-old light-grown seedlings on control or ascorbate-supplemented horizontal plates were imaged and length was quantified using FIJI. Bar charts represent mean values and error bars their corresponding standard deviations. Different letters denote statistically significant differences between mean values (One-Way ANOVA, Tukey post-hoc test, $\alpha=0.05$, $n>10$). Data was transformed using logarithm to meet homoscedasticity (Levene's test) and power >0.8 prior to perform ANOVA



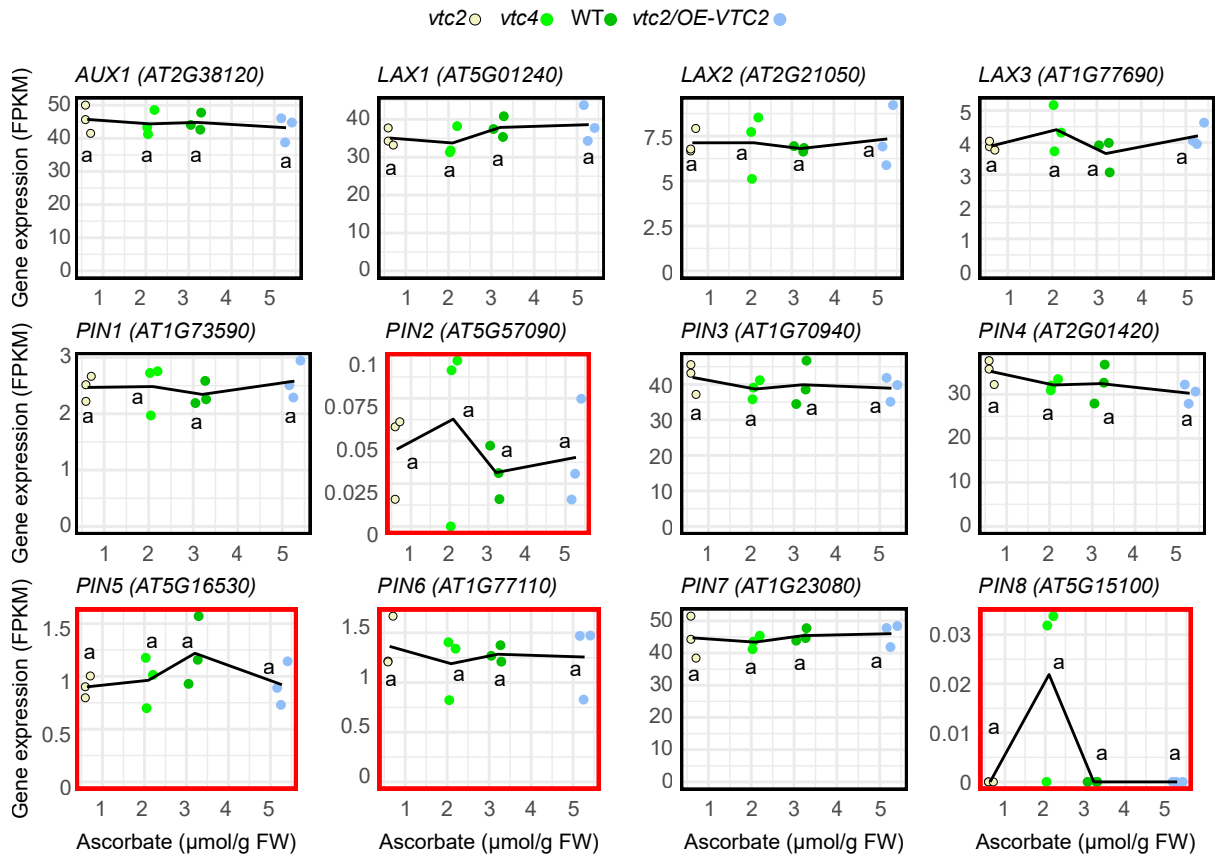
Supplementary Figure S12. Root sensitivity to ascorbate does not rely on an ascorbate-induced H₂O₂ accumulation. A) Spatial accumulation of H₂O₂ in primary root cells in response to exogenous ascorbate (0.5 mM). Top: representative pictures show bright field (left) and their corresponding 8-bit spectrum look-up table (LUT) (right) of root tip microscopy images. Root apical meristem (RAM) comprised the root tip portion from the columella until the first elongating cell of the root tip (not included). Transition zone (TZ) encompassed root cells with increasing length until 340 μm after the end of the RAM (corresponding to the region examined for TAA1 (TRYPTOPHAN AMINOTRANSFERASE OF ARABIDOPSIS 1) accumulation and change in *DR5* activity upon ascorbate supplementation). Bottom: DAB (3,3'-diaminobenzidine) staining intensity in RAM and TZ of Arabidopsis primary roots represented in (A top). Stacked columns represent average DAB staining intensity and standard deviation (AU: arbitrary unites). Individual root staining was quantified using color deconvolution in FIJI (see methods section). Dark: 3-day-old etiolated roots. Light: 5-day-old roots grown under continuous light. All seeds were germinated on AT (control) or on ascorbate-supplemented AT horizontal plates (agar 6 g/L). There were not statistically significant differences in DAB staining of RAM (a) or TZ (a') across light regimes or treatments (Two-Way ANOVA, Tukey post-hoc test, α=0.05, n>6). Data was transformed using logarithm to meet homoscedasticity (Levene's test) and power>0.8 prior to perform ANOVA. Differences between root zones were not tested. Scale bar = 100 μm. B) Relative root length of 5-day-old ascorbate-altered lines grown under continuous light. Green horizontal bars represent the mean value of the population represented with black dots and different letters denote statistically significant differences between mean values (One-Way ANOVA, Tukey post-hoc test, α=0.05). Sample sizes for ascorbate-treated plants are shown at the bottom of the plot; numbers in brackets denote the corresponding control sample sizes used for normalization.



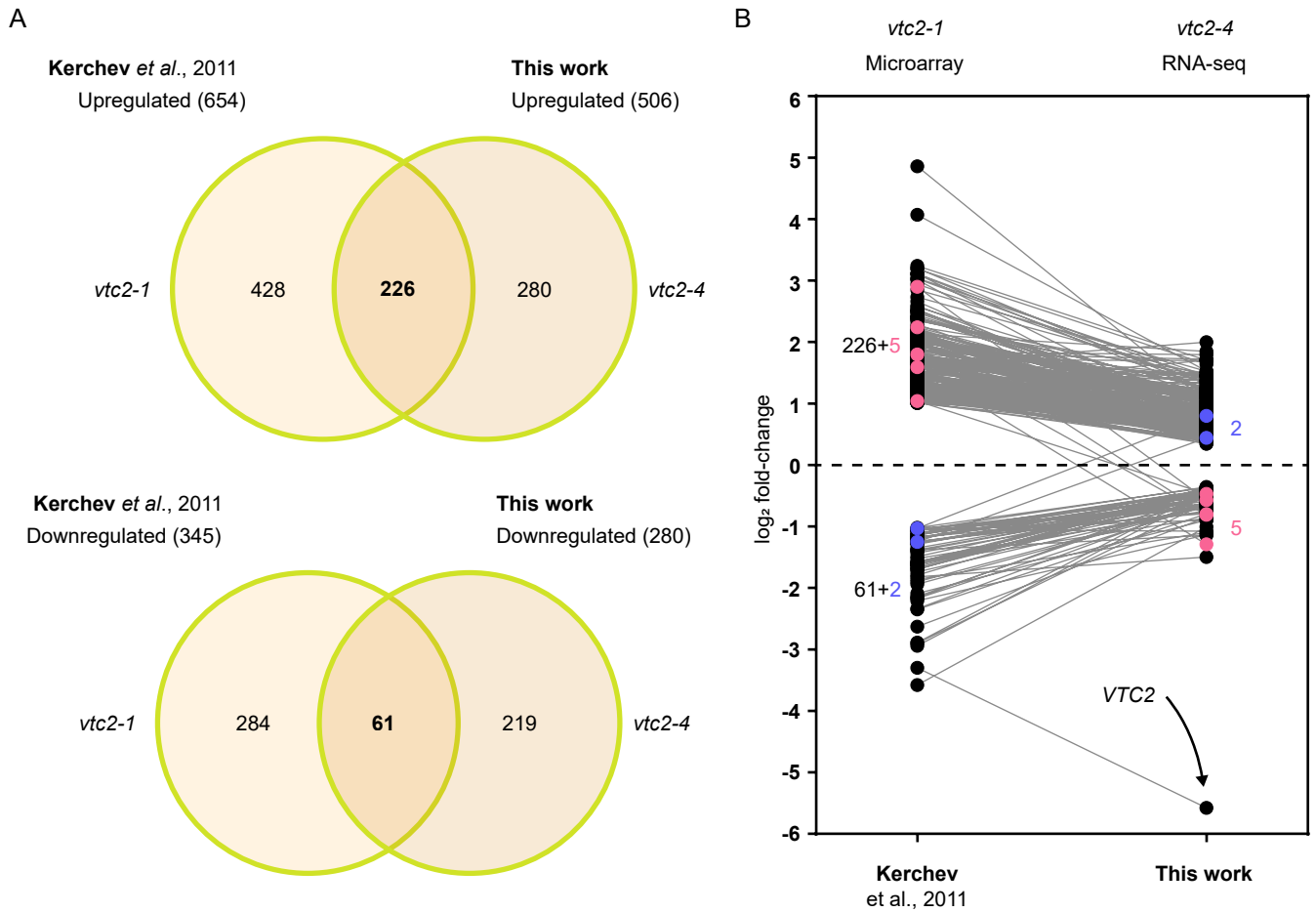
Supplementary Figure S13. Ascorbate supplementation alters the expression patterns of auxin biosynthesis genes *YUCCA5* (*YUC5*), *YUC6*, and *YUC8* in roots of light-grown seedlings and of *YUC3* in roots of dark-grown seedlings. A,B) Arabidopsis lines expressing recombineering-generated GUS translational fusions of *YUCCA* genes (Brumos et al., 2020) were grown for 5 days under continuous light (A) and for 3 days in the dark (B) and stained for GUS. 1-mm scale bar is applicable to all cotyledon images within the panel, and 100-μm scale bar is applicable to all root images within the panel. Scale bars in cotyledon details of panel A for *YUC1* and *YUC6* represent 100 μm.



Supplementary Figure S14. Auxin-deficient double mutant *weī8 tar2* is severely impaired in tryptophan aminotransferase activity, translating into exaggerated shortening of the root in the presence of ascorbate and ectopic overproduction of auxin by *sur2* mutant cannot compensate for defective TAA1-mediated biosynthesis in *weī8 sur2* mutant. A) Representative pictures of auxin-altered lines in response to exogenously applied ascorbate (0.5 mM). Scale bar is the same for all pictures within the panel. Arabidopsis seedlings were germinated and grown for 5 days under continuous light. *weī8-1 tar2-1* mutant and auxin overproducing lines (*YUCox*, *sur2*, and *weī8-1 sur2*) were grown side-by-side with wild-type (WT), *weī8-1*, and the two *tar1 tar2* seedlings displayed in Figure 5 and, therefore, they were also included here for reference. B) Ascorbate-mediated root shortening is associated to smaller root apical meristem, (RAM) size (pointed by blue arrowheads) and altered root hair development. Scale bar is the same for all pictures within the panel. C) Root length comparison between control conditions and ascorbate supplemented treatment (0.5 mM) in auxin-altered lines represented in (A) and (B). Horizontal lines across datapoints represent mean values. Different letters denote statistically significant differences, analyzed by ANOVA of Aligned Rank Transformed Data (2-way ANOVA on ranks, $\alpha=0.05$). Sample sizes for control populations are shown at the bottom of the plot in black whereas ascorbate-treated sample sizes are shown green.



Supplementary Figure S15. Expression profiles of genes encoding auxin import (*AUX1*, *LAX1-LAX3*) and export (*PIN1-PIN8*) carriers in four-week-old Arabidopsis rosettes. RNA-seq Fragments Per Kilobase of transcript per Million mapped reads (FPKM) (y-axes) vs ascorbate concentrations (x-axes) are plotted. Plots for genes with very low expression values (FPKM<1) are framed in red and should not be considered reliable. Different letters denote statistically significant differences (One-Way ANOVA, Tukey post-hoc test, $\alpha=0.05$, $n=3$). Distributions were tested to meet normality (Shapiro–Wilk’s test) and homoscedasticity (Levene’s test) prior to ANOVA. If not meeting any of these requirements, data was transformed using logarithm and, if meeting the requirements, proceeded to perform ANOVA. Otherwise, Kruskal-Wallis followed by Dunn’s post-hoc test were performed. FW: fresh weight. *AUX1*: *AUXIN RESISTANT1*, *LAX*: *LIKE AUXIN RESISTANT*, *PIN*: *PIN-FORMED*.



Supplementary Figure S16. Comparison of *vtc2*-regulated gene lists identified in this work and that published by Kerchev et al. (2011). A) Overlap between upregulated or downregulated genes identified in *vtc2-1* (EMS allele, microarray; Kerchev et al., 2001) and *vtc2-4* (T-DNA allele, RNA-seq; this work). B) Expression fold-change of overlapping genes between the two compared studies (266 upregulated, and 61 downregulated) including DEGs whose fold change is reversed between studies: in pink, 5 genes that were upregulated in Kerchev's study were downregulated in ours; In blue, 2 genes that were downregulated in Kerchev's study were upregulated in ours. Data available in Supplementary Dataset S10.